

Polar cap potential saturation during large geomagnetic storms

J. Raeder^{a,*}, G. Lu^b

^a Institute of Geophysics and Planetary Physics, University of California, Los Angeles, 405 Hilgard Avenue, Los Angeles, CA 90095-1567, USA

^b NCAR/HAO, P.O. Box 3000, Boulder, CO 80307, USA

Received 6 January 2003; accepted 20 May 2004

Abstract

We present evidence that the cross polar cap potential saturates during the Bastille Day geomagnetic storm which is characterized by large values of the driving interplanetary electric and magnetic fields. Empirical models that were derived and constrained for more benign solar wind conditions severely over-predict the cross polar cap potential for this event. Global simulation results show that the magnetopause moves significantly inward as a result of compression and erosion of the magnetosphere. We propose a model that explains the potential saturation primarily as an effect of the shortened x -line. An appropriately modified empirical model gives much better potential prediction, supporting our hypothesis.

© 2005 Published by Elsevier Ltd on behalf of COSPAR.

Keywords: Large geomagnetic storms; Polar cap potential saturation; Global simulation

1. Introduction

The ionosphere potential patterns in Earth's polar caps are of fundamental importance for magnetospheric physics. They reflect the convection state of the magnetosphere which is very difficult to measure using in situ observations because of a lack of sufficient data. However, the polar cap potential pattern can be estimated with fairly high accuracy and at high spatial and temporal resolution using measurements from low Earth orbiting satellites (Papitashvili et al., 1999; Hairston et al., 1999), from radars (Ruohoniemi and Greenwald, 1995; Greenwald et al., 1999; Shepherd et al., 1999), from ground magnetometers (Kamide et al., 1981), or from a combination thereof using assimilative techniques (Richmond, 1992; Richmond et al., 1997, 1998; Lu et al., 1994, 1995; Knipp, 1993). An even simpler measure of the ionospheric and magnetospheric convection

state can be obtained from the cross polar cap potential (CPCP), that is, the difference between the maximum and the minimum of the potential in one hemisphere. Because there are in general more measurements available from the northern polar cap, we discuss in this paper only northern hemisphere data model results; relatively little is known about the relation between the potential differences between the hemispheres (Lu et al., 1994).

The relation of the CPCP to the driving of the solar wind and the IMF has been extensively studied (Boyle et al., 1997; Doyle and Burke, 1983; Reiff et al., 1985, 1981; Burke et al., 1999). Most of these studies are based on regression analysis of measured CPCP versus driving parameters in the solar wind. Generally, the strongest correlations are those with the IMF B_z component and with the interplanetary electric field (IEF) component E_y ($=V_{SW} \times B_z$), with minor contributions from the solar wind dynamic pressure, velocity, and density. Improved correlations are found if the rectified IMF B_z is used, i.e., if the contribution of a northward IMF is discarded. For northward IMF, the models then predict a

* Corresponding author. Tel.: +1 603 862 3412; fax: +1 603 862 3584.
E-mail address: j.raeder@unh.edu (J. Raeder).

“quiet time” or “baseline” CPCP that is of the order of at most a few 10 s of kV. The correlations always exhibit a lot of scatter and the correlation coefficients rarely exceed values ~ 0.8 . The relatively poor correlation between the CPCP and the SW/IMF parameters may be due to a number of reasons, including uncertainties of the CPCP estimation, difficulty in estimating the correct SW/IMF condition because of less-than-optimal solar wind monitor locations, time delays in the ionospheric response (Bargatze et al., 1985), or simply because there is no linear response of the CPCP to changing solar wind and IMF conditions.

More recently, attention has been drawn to the SW/IMF–CPCP relationship during periods of very strong forcing, that is, during geomagnetic storms. Although some earlier studies had indicated that the CPCP may saturate during periods of strong forcing (Reiff et al., 1981; Reiff and Luhmann, 1986), other studies did not confirm saturation effects (Boyle et al., 1997) and thus the topic remains controversial.

More recently, Russell et al. (2001), re-analyzing data published by Burke et al. (1999) showed that more recent storms clearly exhibited CPCP saturation. This study indicated that a saturation effect may occur for values of the IEF as low as 3 mV/m, however, the data used in this study exhibit a large amount of scatter and also seem to be consistent with a larger saturation threshold. Siscoe et al. (2002) have attempted to explain the potential saturation using a modified version of the Hill model of the transpolar potential (Hill et al., 1976; Hill, 1984) which predicts that the CPCP limitation is caused by the ram-pressure limited region 1 current system which in the case of saturation replaces the Chapman–Ferraro currents to provide the $\mathbf{J} \times \mathbf{B}$ force balance at the magnetopause. They also compare this theoretical model with results from the ISM global magnetosphere model and find a good agreement between the two models. They do not, however, compare the model predictions with any data or with empirical models.

The current solar maximum now offers a plethora of new geomagnetic storm data which allow us for the first time to perform much more detailed comparisons between the data and models. In particular, we have now data at hand that cover extreme solar wind driving conditions. In this study, we pick one of these events (the so-called Bastille Day storm of July 14/15 2000), analyze its geomagnetic impact and compare with the results from our global model. Based on these comparisons, we offer a new model of CPCP saturation and discuss its relation with the existing models.

2. The Bastille Day storm

The Bastille Day storm is one of the “great” storms of this cycle maximum with a peak D_{ST} value of about

–300 nT. It also stands out because the IMF reaches very strong negative values of up to –60 nT and the interplanetary electric field (IEF) reaches values of up to 70 mV/m. In Fig. 1, we compare this storm with 11 other storms of the 1998–2000 time period. The values of D_{ST} , IME E_y , IMF B_z , and the dynamic pressure are plotted in ‘epoch’ fashion, where the epoch time is chosen to be the onset of the storm main phase as seen in the top panel. Values for the Bastille Day storm are plotted as black lines, whereas the values for the other storms are plotted in light gray without specific distinction between these storms. The main purpose of this figure is to put the Bastille Day storm into context and to show that, although its D_{ST} values are roughly comparable to the other storms, both E_y and B_z are significantly larger compared to the other storms. This figure also shows that the dynamic pressure of the solar wind during the Bastille Day storm is not significantly different, in particular during the main phase.

Fig. 2 shows in the top panel the IMF B_z for the Bastille Day storm, in the middle panel the CPCP from the model (gray line) and from AMIE (black line), and in the bottom panel the AU and AL indices computed from a large number of auroral zone magnetometers. Again, the model predictions are shown with a gray line and the data with a solid black line. The predicted AU and AL indices are computed using first principles,

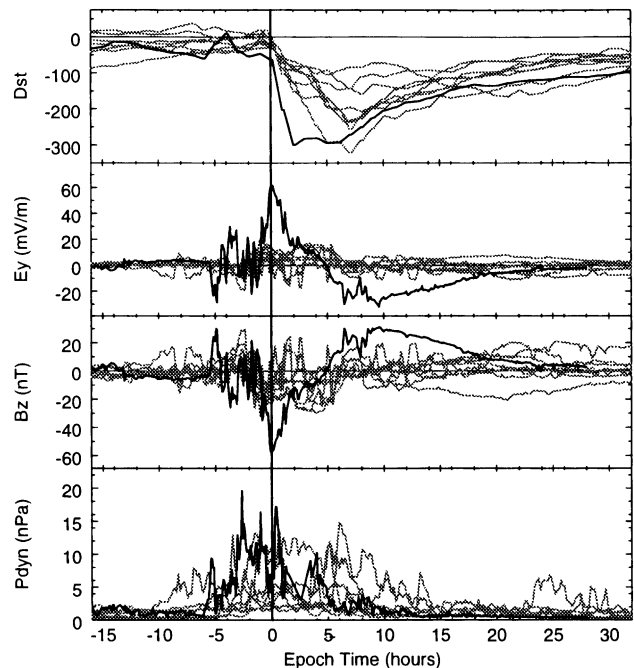


Fig. 1. The Bastille Day storm (black lines) in relation to other storms in the 1998–2000 period (gray lines). The epoch time is chosen to be the onset of the storm main phase. From top to bottom: The D_{ST} index, the interplanetary electric field E_y component, the IMF B_z component, and the dynamic pressure of the solar wind.

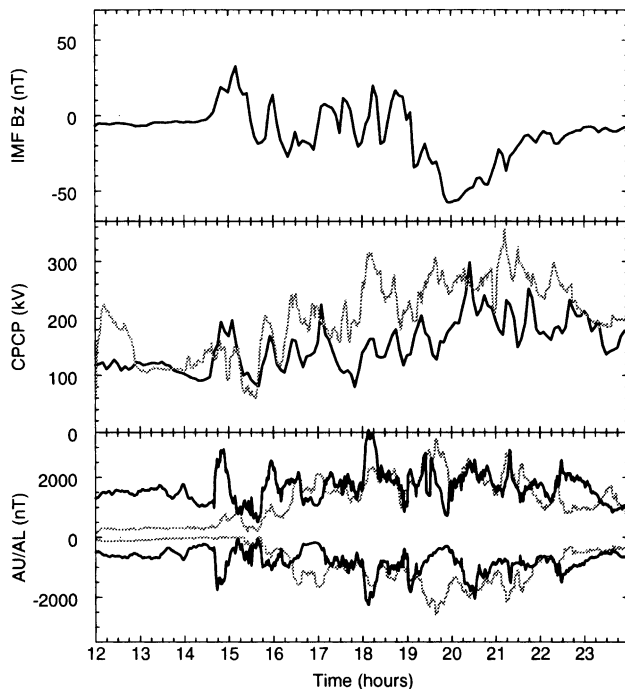


Fig. 2. IMF B_z and geomagnetic activity of the Bastille Day storm. Second panel: polar cap potential from the model (gray) and from AMIE (black). Bottom panel: AL and AU indices from the model (gray) and observed (black).

i.e., using Biot–Savart’s law for a number of auroral stations (see Raeder et al. (2001a) for details.) The main characteristics of this storm are: (i) the storm sudden commencement (SSC) around 1430 UT that signals the arrival of the leading interplanetary shock, (ii) the sheath of the interplanetary coronal mass ejection (ICME) between 1430 and 1930 UT, and (iii) the ICME proper, starting at ~ 1930 UT. The IMF is already long before the SSC strongly southward oriented and thus possibly preconditioning the magnetosphere. The ICME sheath is characterized by large excursions of the IMF B_z and B_y (not shown here) with amplitudes of about 20 nT. In the ICME proper, the IMF rotates quickly to about -60 nT (due south) at 2000 UT and afterward slowly towards a more northward orientation. Comparing the first two panels it is obvious that the CPCP does not follow the IMF B_z very closely. Although there is some degree of anti-correlation between the curves, simple visual inspection does not indicate a strong correlation as one would expect from the empirical models. The match between the data and the model predictions is reasonable, both for the CPCP and the auroral indices. The model predicts somewhat higher CPCP values, but basically stays within the bounds of observed values. The same is true for the AU and AL values. Here, the model predicts a good fraction of the individual ‘onsets’ and the disturbance levels are comparable to the observed ones (see Raeder et al. (2001b) for details).

3. Potential saturation

In Fig. 2, it is obvious that there is no good correlation between the IMF B_z or the IME E_y (the solar wind velocity is fairly constant at ~ 1100 km/s, not shown here) and CPCP. Consequently, we expect that most of the empirical models will not provide very accurate predictions of the CPCP. This is shown in Fig. 3, which displays the predicted CPCP from three of these models (Boyle et al., 1997; Doyle and Burke, 1983; Reiff et al., 1981) and the prediction from our global MHD model versus the AMIE CPCP estimates. The black line in this figure has unit slope indicating the perfect prediction. There is significant scatter of the predicted values in all of the models which is probably due to the possible reasons given in Section 1. However, there is also a systematic over prediction of the CPCP for all of the models, in some cases by more than a factor of 6. The Figure also shows the RMS error for the various models. The Reiff et al. (1981) model and the global MHD model show the least scatter and predict a limitation of the CPCP values at 400 and 350 kV, respectively. The Reiff et al. model has such a limitation built in (Reiff et al., 1981) in an empirical fashion, while the MHD model produces the limitation self-consistently as we shall see in the following. The other models do not limit the CPCP in any way which thus leads to extreme and unrealistic predicted CPCP values. The largest CPCP values that are typically observed lie in the 250–300 kV range, while the model predictions are as large as 1400 kV. In fairness to these models we note, however, that these models were never designed or constrained for such driving

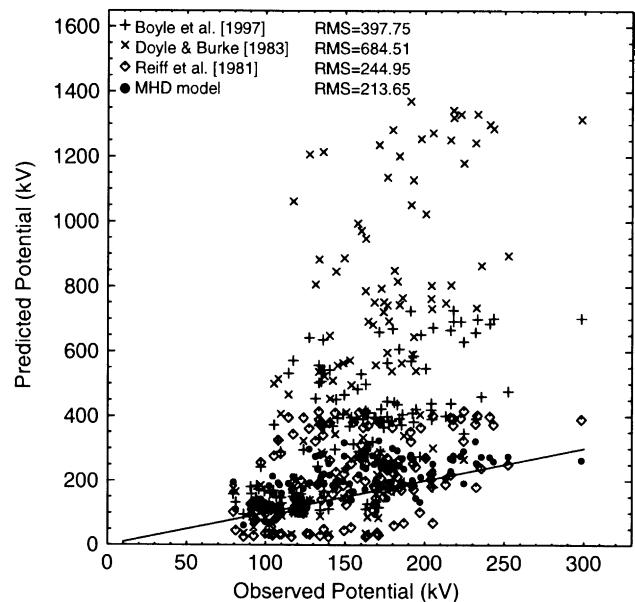


Fig. 3. Various model predictions of the CPCP during the Bastille Day storm versus the observed (AMIE estimated) CPCP. ‘RMS’ is the root mean square error.

conditions. Thus, applying them to such conditions puts them way out of their range of validity. Inspecting the predictions of these models for such extreme conditions is, however, instructive because it shows that a seemingly linear relationship that holds well for typical benign conditions should not be extrapolated. It also points us to the importance of understanding the underlying physical processes in constructing predictive models.

4. Saturation process

The simplest model of solar wind–ionosphere coupling is that during southward IMF conditions, reconnection at the dayside magnetopause opens a window that allows open field lines to connect from the ionosphere directly to the solar wind. In steady state, then, the electric field would directly map from the solar wind into the ionosphere (Kelley, 1989). In reality, this mapping would be affected by the reconnection efficiency f that reduces the electric field that actually acts on the ionosphere. This solar wind–ionosphere coupling process may equivalently be expressed in terms of stresses and flows (Parker,

1996; Strangeway et al., 2000), but for the sake of simplicity we will stick with the electrodynamic description here. The CPCP $\Delta\Phi$ may then be expressed as: $\Delta\Phi \sim L \times E$, where L is the length of the x -line and E the electric field at the x -line. Because L is proportional to the magnetopause distance from Earth R_{MP} and because E is proportional to the IME E_y , we may also write:

$$\Delta\Phi = f \times R_{MP} \times E_y, \tag{1}$$

where we have lumped the proportionality constants into the factor f .

Fig. 4 shows the magnetopause (MP) distance R_{MP} from the MHD model as a function of time for the period of interest. The magnetopause moves very close to Earth, in particular during the storm main phase. The simulation result is very realistic, it has been shown to match the magnetopause crossings of 3 geostationary GOES satellites very closely (Raeder et al., 2001a). Both MP erosion (Shue et al., 2001) and compression contribute to the close MP distance. However, because the dynamic pressure is not so much elevated erosion seems to be the main factor. Thus, if Eq. (1) holds, the saturation of the x -line by magnetopause erosion. In order to test this hypothesis, we have scaled the Boyle CPCP model by R_{MP}/R_0 , where $R_0 = 11R_E$ is the nominal MP distance. We have chosen the Boyle model because it is based on the largest statistical data set and because it shows the best correlation between the observed and the predicted CPCP when there is no CPCP saturation.

The result with the scaled Boyle model is shown in Fig. 5, along with the MHD model results. Clearly, the Boyle model is much improved by this scaling and its RMS error is now much closer to that of the MHD model. Thus, the shortening of the x -line does indeed seem to play a major role in CPCP saturation.

5. Summary and discussion

We have shown that at least for one event, the Bastille Day Storm, CPCP saturation occurs. This is

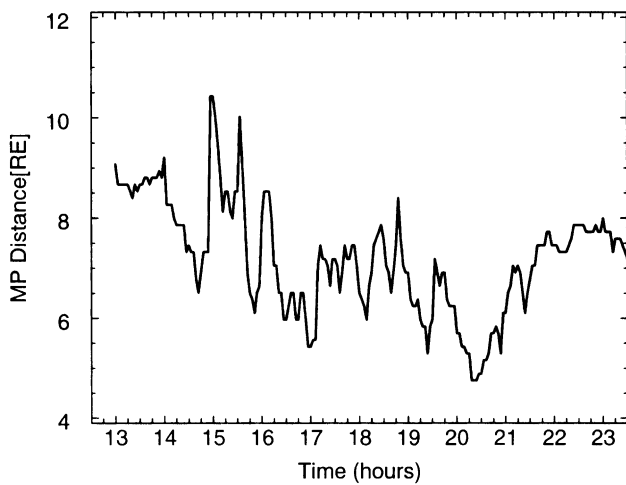


Fig. 4. The subsolar magnetopause distance on July 15, 2000 as derived from the model.

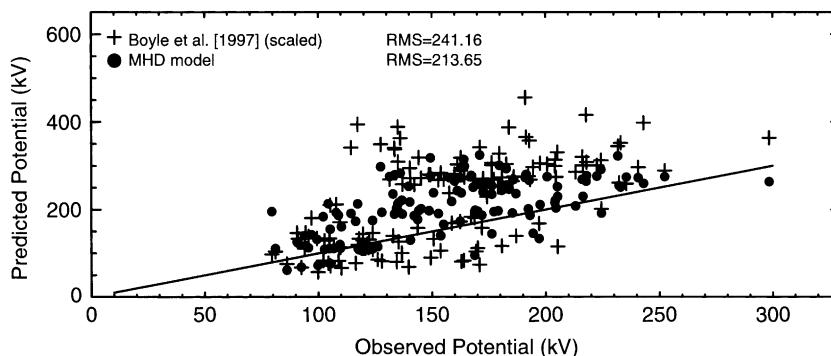


Fig. 5. Predicted CPCP with the scaled Boyle model versus the AMIE CPCP estimates.

evident both from the data and from a MHD simulation. Most empirical CPCP models were never designed or constrained for such extreme events as this storm. Thus, they produce CPCP predictions that are much too large. The MHD model results indicate that a simple geometrical effect, that is, shortening of the dayside x -line due to magnetopause erosion and compression may explain, at least in part, this saturation effect. We have tested this hypotheses by appropriately scaling the Boyle model. Such scaling does indeed improve the prediction efficiency of that model substantially, thus underpinning our hypothesis. With respect to Siscoe's model (Siscoe et al., 2002) we note that our model is not in contradiction to their model. Compression and erosion of the magnetopause does indeed increase the region 1 currents as the Siscoe model predicts. An interesting question is how other predictions of our model and the Siscoe model compare. For example, our model also predicts that the CPCP should decrease with increasing SW dynamic pressure and all other parameters being equal. The Siscoe model predicts exactly the opposite. These predictions may be difficult to test using data because the dynamic pressure dependence is fairly weak and may be masked by fluctuations in the data. Global simulations, however, may be able to answer some of these questions.

Acknowledgements

This work was supported by NASA Grant NAG 5-10986 and NSF Grant ATM-00-84483 at UCLA. Global MHD model runs were performed using the National Partnership for Advanced Computational Infrastructure (NPACI) resources.

References

- Bargatze, L., Baker, D.N., McPherron, R.L., Hones, E.W. Magnetospheric impulse response for many levels of geomagnetic activity. *J. Geophys. Res.* 90, 6387–6394, 1985.
- Boyle, C.B., Reiff, P.H., Hairston, M.R. Empirical polar cap potentials. *J. Geophys. Res.* 111, 102–126, 1997.
- Burke, W.J., Weimer, D.R., Maynard, N.C. Geoeffective interplanetary scale sizes derived from regression analysis of polar cap potentials. *J. Geophys. Res.* 104, 9989–9994, 1999.
- Doyle, M.A., Burke, W.J. S3-2 measurements of the polar cap potential. *J. Geophys. Res.* 88, 9125–9133, 1983.
- Greenwald, R.A., Ruohoniemi, J.M., Baker, K.B., Bristow, W.A., Sofko, G.J., Villain, J.P., Lester, M., Slavin, J. Convective response to a transient increase in dayside reconnection. *J. Geophys. Res.* 104, 10007–10016, 1999.
- Hairston, M.R., Weimer, D.R., Heelis, R.A., Rich, F. Analysis of the ionospheric cross polar cap potential drop and electrostatic potential distribution patterns during the January 1997 cme event using dmsp data. *J. Atmos. Sol. – Terr. Phys.* 61, 195–206, 1999.
- Hill, T.W. Magnetic coupling between solar wind and the magnetosphere: regulated by ionospheric conductance? *Eos Trans. AGU* 65, 1047, 1984.
- Hill, T.W., Dessler, A.J., Wolf, R.A. Mercury and mars: The role of ionospheric conductivity in the acceleration of magnetospheric particles. *Geophys. Res. Lett.* 3, 429–432, 1976.
- Kamide, Y., Richmond, A.D., Matsushita, S. Estimation of ionospheric electric fields, ionospheric currents, and field-aligned currents from ground magnetic records. *J. Geophys. Res.* 86, 801–813, 1981.
- Kelley, M.C. *The Earth's Ionosphere*. Academic Press, New York, 1989.
- Knipp, D.J. Ionospheric convection response to slow, strong variations in a northward interplanetary magnetic field: a case study for January 14, 1988. *J. Geophys. Res.* 98, 19273–19292, 1993.
- Lu, G. et al. Interhemispheric asymmetry of the high latitude convection pattern. *J. Geophys. Res.* 99, 6491–6510, 1994.
- Lu, G. et al. Characteristics of ionospheric convection and field-aligned current in the dayside cusp region convection pattern. *J. Geophys. Res.* 100, 11845–11862, 1995.
- Papitashvili, V.O., Rich, F.J., Heinemann, M.A., Hairston, M.R. Parameterization of the defense meteorological satellite program ionospheric electrostatic potentials by the interplanetary magnetic field strength and direction. *J. Geophys. Res.* 104, 177–184, 1999.
- Parker, E.N. The alternative paradigm for magnetospheric physics. *J. Geophys. Res.* 101, 10587–10626, 1996.
- Raeder, J., Wang, Y.L., Fuller-Rowell, T.J., Singer, H.J. Global simulation of space weather effects of the Bastille Day storm. *Sol. Phys.* 204, 325–336, 2001a.
- Raeder, J. et al. Global simulation of the geospace environment modeling substorm challenge event. *J. Geophys. Res.* 106, 381–395, 2001b.
- Reiff, P.H., Luhmann, J.G. Solar wind control of the polar cap potential. in: Kamide, Y., Slavin, J.A. (Eds.), *Solar Wind – Magnetosphere Coupling*. Terra Scientific Publishing Company, Tokyo, pp. 453–468, 1986.
- Reiff, P.H., Spiro, R.W., Hill, T.W. Dependence of polar cap potential drop of interplanetary parameters. *J. Geophys. Res.* 86, 7639–7648, 1981.
- Reiff, P.H., Spiro, R.W., Wolf, R.A., Kamide, Y., King, J.H. Comparison of polar cap potential drops estimated from solar wind and ground magnetometer data: CDAW 6. *J. Geophys. Res.* 90, 1318–1324, 1985.
- Richmond, A.D. Assimilative mapping of ionospheric electrodynamics. *Adv. Space Res.* 6 (1), 59–68, 1992.
- Richmond, A.D., Lu, G., Emery, B.A., Lummerzheim, D., Parks, G.K. Analysis of large scale electro-dynamic features of the high latitude ionosphere during substorms (abstract), in: 8th Assembly, International Association for Geomagnetism and Aeronomy, Rockville, MD, p. 323, 1997.
- Richmond, A.D., Lu, G., Emery, B.A., Knipp, D.J. The AMIE procedure: prospects for space weather specification and prediction. *Adv. Space Res.* 22, 103–112, 1998.
- Ruohoniemi, J.M., Greenwald, R.A. Observations of IMF and seasonal effects in high-latitude convection. *Geophys. Res. Lett.* 22, 1121–1124, 1995.
- Russell, C.T., Luhmann, J.G., Lu, G. Non-linear response of the polar ionosphere to large values of the interplanetary electric field. *J. Geophys. Res.* 106, 18495–18498, 2001.
- Shepherd, S.G., Greenwald, R.A., Ruohoniemi, J.M. A possible explanation for rapid, large-scale ionospheric responses to southward turnings of the IMF. *Geophys. Res. Lett.* 26, 3197–3200, 1999.
- Shue, J.H., Song, P., Russell, C.T., Thomsen, M.F., Petrinec, S.M. Dependence of magnetopause erosion on southward interplanetary magnetic field. *J. Geophys. Res.* 106, 18777–18788, 2001.
- Siscoe, G.L., Crooker, N.U., Siebert, K.D. Transpolar potential saturation: roles of region 1 current system and solar wind ram pressure. *J. Geophys. Res.* 107, 1321–1328, doi:10.1029/2001JA009176, 2002.
- Strangeway, R.J., Russell, C.T., Carlson, C.W., McFadden, J.P., Ergun, R.E., Temerin, M., Klumpar, D.M., Peterson, W.K., Moores, T.E. Cusp field-aligned currents and ion outflows. *J. Geophys. Res.* 105, 21129–21142, 2000.